Two-Vector Dimensionless Model Predictive Control of PMSM Drives Based on Fuzzy Decision Making

Nabil Farah, Gang Lei, *Member, IEEE*, and Jianguo Zhu, *Senior Member, IEEE*, and Youguang Guo, *Senior Member, IEEE*

***Abstract*— Model predictive controls (MPCs) with the merits of non-linear multi-variable control can achieve better performance than other commonly used control methods for permanent magnet synchronous motor (PMSM) drives. However, the conventional MPCs have various issues, including unsatisfactory steady-state performance, variable switching frequency, and difficult selection of appropriate weighting factors. This paper proposes two different improved MPC methods to deal with these issues. One method is the two-vector dimensionless model predictive torque control (MPTC). Two cost functions (torque and flux) and fuzzy decision-making are used to eliminate the weighting factor and select the first optimum vector. The torque cost function selects a second vector whose duty cycle is determined based on the torque error. The other method is the two-vector dimensionless model predictive current control (MPCC). The first vector is selected the same as in the conventional MPC method. Two separate current cost functions and fuzzy decision-making are used to select the second vector whose duty cycle is determined based on the current error. Both proposed methods utilize the space vector PWM modulator to regulate the switching frequency. Numerical simulation results show that the proposed methods have better steady-state and transient performances than the conventional MPCs and other existing improved MPCs.**

***Index Terms*—electrical drives, permanent magnet synchronous motors, model predictive control.**

I. Introduction

PERMANENT magnet synchronous machines (PMSMs) with high power density, high efficiency, higher torque, and less electrical losses are widely used in various applications. To meet different application requirements, electrical machine controls or drives have been introduced [1]. For decades, field-oriented control and direct torque control have been the two popular high-performance control schemes for PMSM drives [2-4]. Recently, model predictive control (MPC) methods have been proposed as a better control method for electrical drives with the merits of conceptual simplicity, easy implementation, non-linearity, and multi-variable control [5, 6]. In the last decade, MPC has received extensive interest in the field of electrical drives with various MPC methods developed for induction motors [7, 8], PMSMs [9, 10], switched reluctance motors [11], and other types of electrical machines [12].

Based on the control variables, the most common MPCs are the model predictive torque & flux control (MPTC), which uses the torque and flux as the control variables, and the model predictive current control (MPCC), which uses the stator currents as the control variables [13, 14]. They predict their future behaviors and select an optimum switching vector by minimizing their cost functions based on their control variables [15]. The conventional MPCs apply the vector chosen for the whole control cycle, which is inadequate to regulate the torque and may result in an unsatisfactory steady-state performance [16]. The finite control set MPC (FCS-MPC) generates the switching pulses directly, and the switching frequency of the power electronic converter is variable, a significant concern in MPC. Variable switching frequency results in high current and voltage ripples, creating an audible noise and degrading the drive system's steady-state performance [17, 18].

On the other hand, MPC with different control variables in magnitude and unit (i.e., torque and flux) requires selecting a proper weighting factor to balance them [19]. The weighting factor selection is ambiguous due to the lack of systemic selection guidance. An inappropriate weighting factor can result in high torque ripples in MPTC [20].

Various improvements have been proposed to deal with these issues of conventional MPCs; for instance, additional vectors are applied along with the optimum vector during a control cycle. More than one vector-based MPCs have been reported to increase the stability of the motor drives, improve the steady-state performance, and reduce the torque and current ripples [21]. Two-vector-based MPCC for PMSM drives with vector duration control was proposed in [16]. The first vector is selected in a similar way to the conventional MPC. The second vector is among the adjacent vectors to the first optimum vector to ensure only one change of switching state at each control

Manuscript received November 02, 2022; accepted December 10, 2022. date of publication December 25, 2022; date of current version December 18, 2022.

Nabil Farah is with the School of Electrical and Data Engineering University of Technology Sydney (UTS), NSW 2007, Australia (email:nabil.farah@student-.uts.edu.au).

Gang Lei and Youguang Guo are with the School of Electrical and Data Engineering, University of Technology Sydney, NSW 2007, Australia (e-mail: Gang.Lei@uts.edu.au, Youguang.Guo-1@uts.edu.au).

Jianguo Zhu is with the School of Electrical and Information Engineering, University of Sydney, NSW, 2006, Australia (e-mail: jianguo.zhu-@sydney.edu.au).

(Corresponding Author: Nabil Farah)

Digital Object Identifier 10.30941/CESTEMS.2022.00029

cycle to avoid high switching frequency. In [22], a three-vector MPCC for PMSM drives based on the space vector modulation (SVM) technique was proposed. This method evaluates the cost function for three voltage vectors, calculates their durations, and then applies them in one control cycle. Unlike [16], this method first evaluates the cost function to obtain the optimal vector and calculate its duration. Then, it selects the second vector from a combination of two adjacent active vectors to the first vector and zero vector and applies it for the rest of the duration.

A two-vector-based MPCC of PMSM drives was proposed in [23] to improve the steady-state performance. Firstly, a reference vector is calculated based on deadbeat current control, and the first optimum vector is selected as the nearest active to the reference vector. The second vector is chosen among the three candidates to be two adjacent active vectors to the first vector or a zero vector, such that a candidate with minimal distance from the reference vector is selected. Unlike other two-vector MPCs, this method does not require the calculation of the current slope to obtain the vector duration.

The selection of the weighting factor can significantly impact the drive performance, and a fixed value weighting factor might not be adequate for a wide operation range. The weighting factor can be optimized manually (offline) through an empirical trial and error procedure [24] or some other methods, such as parameter sweep [25] and Genetic algorithm [26]. However, these methods are time-consuming and prone to the influences of parameters and operating conditions [27]. Many different approaches have been attempted to obtain an appropriate weighting factor. In [28], an MPTC with no weighting factor was proposed for PMSM drives. The cost function is based on the voltage vector tracking error instead of the torque and flux errors. The principle of deadbeat-direct torque&flux control was employed to obtain the reference voltage vector to ensure that the torque and flux errors converge to zero. Based on a similar principle, [29] proposed an MPTC with a voltage vector cost function for PMSM drives. In [30], the weighting factor was eliminated from the predictive torque control for PMSM drives using a lookup table of direct torque control. Only three voltage vectors are predicted and evaluated in the cost function.

Variable switching frequency is a significant concern in MPC, which generates high current and voltage ripples, resulting in audible noise and deteriorating the system's steady-state performance [17, 18, 31]. Switching frequency regulation techniques have been introduced in MPC to overcome the issue of the variable switching frequency. Common-mode voltage (CMV) suppression is one of the techniques used to regulate the switching frequency of conventional MPC methods for PMSM drives. CMV is the voltage between the midpoint DC-link capacitor and the neutral point of the load. A high-frequency CMV can increase the leakage current and electromagnetic interface, damaging the motor shaft. [33] proposed an MPC with constant switching frequency to suppress the CMV in PMSM drives. Compared to the conventional MPC, where only one active vector is applied, this method applies four active vectors in the next control cycle. The switching sequence model is developed to keep the switching frequency fixed and equal to the control frequency. This method applies the principle of 4 active voltage vectors where the zero vector is avoided to restrict the amplitude of CMV, and two non-adjacent vectors are used to create the equivalent zero vector. With a total prohibition of zero vector, the CMV and switching frequency can be decreased, but the current signal quality is significantly affected.

All of the issues associated with conventional MPC significantly impact the overall drive performances. Thus, an effective MPC should realize the trade-off between these different issues because focusing on one issue and neglecting the others can degrade the performance over a wide range of operations and various operating conditions. For instance, suppressing the CMV by eliminating the zero vector can regulate the switching frequency but lead to high current distortions and torque ripple. Similarly, two- or three-vector-based MPC can improve torque performance but generate high variable switching frequencies without properly regulating the switching sequence.

This paper proposes two improved MPC methods to deal with different issues of the conventional MPC while maintaining a trade-off between these issues. The first method is based on MPTC, which implements two-vector and two cost functions (torque and flux). The fuzzy decision-making can eliminate the weighting factor and select the first optimum vector. The torque cost function is used to select the second vector whose duty cycle is determined based on torque error to decrease torque ripples further. The second method is based on MPCC with two voltage vectors. The first vector is selected in the same way as in the traditional method. Two separate current cost functions and fuzzy decision-making are used to select the second vector, whose duty cycle is determined based on the current error. Both proposed methods utilize the space vector PWM modulator to regulate the switching frequency.

The rest of the paper is organized as follows. Section II discusses the mathematical modelling of PMSM drive systems with MPC. Section III discusses the proposed MPC methods. Section IV presents the simulation studies and performance comparison of the proposed methods with other methods. Section V summarizes the findings and outcomes of the paper.

II. CONVENTIONAL MPC OF PMSM DRIVES

In order to design an efficient control strategy for PMSM, an accurate mathematical model of the machine is to be developed. A three-phase PMSM can be transformed into the *d-q* equivalent model, and the voltage flux linkage equations of PMSM in the *d-q* frame can be expressed as:

$$v_d = R_s i_d + L_d \frac{di_d}{dt} - \omega L_q i_q \tag{1}$$

$$v_q = R_s i_q + L_q \frac{di_q}{dt} + \omega L_d i_d + \omega \psi_{pm} \tag{2}$$

$$\psi_d = L_d i_d + \psi_{pm} \tag{3}$$

$$\psi_q = L_q i_q \tag{4}$$

where v_d and v_q are the voltages, i_d ?? i_q , L_d ,and L_q are

the currents and the inductances of the *d*- and *q*-axes, respectively.

The dynamic mechanical equation can be expressed as:

$$T_{em} = T_L + J\frac{d\omega}{dt} + B\omega \tag{5}$$

where

$$T_{em} = \frac{3}{2}p\left(\psi_d i_q - \psi_q i_d\right) \tag{6}$$

is the electromagnetic torque, T_L the load torque, J the momentum of inertia, and B the vicious friction coefficient.

Substituting (3) and (4) into (6), one can have

$$T_{em} = \frac{3}{2}p\left[\psi_{pm} i_q + \left(L_d - L_q\right) i_q i_d\right] \tag{7}$$

Based on (1)-(6), different MPC control methods can be constructed for PMSM drives. They can be categorized into two common types based on the controlled variables, MPCC and MPTC. Fig. 1 shows a general block diagram of MPC for PMSM drive, which includes measurement $\left(i_{abc}, \omega_r\right)$, and estimation $\left(\psi_s, T_e\right)$, cost function minimization, and outer speed control loop.

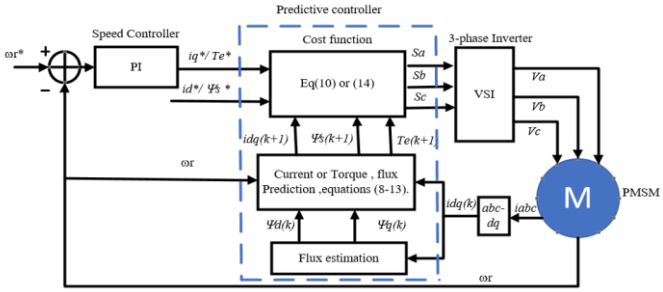

Fig.1. A general block diagram of MPC for PMSM drives.

MPCC obtains the *dq* currents and machine position at sampling instant (*k*). The *dq* voltages are estimated and used to predict the *dq* currents for the next sampling interval (*k*+1). From the PMSM equations (1) and (2), using Euler derivative approximation at sampling time T_s, one can obtain the *dq* currents at time instant (*k*+1) as the following:

$$i_d\left(k+1\right) = \left(1 - \frac{R_s T_s}{L_d}\right) i_d\left(k\right) + \frac{L_q}{L_d} T_s \omega i_q\left(k\right) + \frac{T_s}{L_d} v_d \tag{8}$$

$$i_q\left(k+1\right) = \left(1 - \frac{R_s T_s}{L_q}\right) i_q\left(k\right) - \frac{L_d}{L_q} T_s \omega i_d\left(k\right) - T_s \omega \psi_{pm} + \frac{T_s}{L_q} v_d \tag{9}$$

Then, the MPCC cost function to select the optimum voltage vector from eight voltage vectors ($\left(V_0 - V_7\right)$ of a 2-level three-phase inverter can be expressed as:

$$g_{MPCC} = \left|i_d^* - i_d\left(k+1\right)\right| + \left|i_q^* - i_q\left(k+1\right)\right| \tag{10}$$

MPTC predicts future torque and flux values based on the measured stator currents and rotor speed. From the PMSM flux linkage in (3) and (4), torque in (7), and using the predicted currents in (8) and (9), the predicted flux and torque at the next sampling instant (*k*+1) can be expressed as:

$$\psi_d\left(k+1\right) = L_d i_d\left(k+1\right) + \psi_{pm} \tag{11}$$

$$\psi_q\left(k+1\right) = L_q i_q\left(k+1\right) \tag{12}$$

$$T_{em}\left(k+1\right) = \frac{3}{2}p\left[\psi_{pm}\, i_q\left(k+1\right) + \left(L_d - L_q\right) i_{dq}\left(k+1\right)?\right] \tag{13}$$

The cost function of MPTC to be yielded by an optimum voltage can be expressed as:

$$g_{MPTC} = \left|T_{em}^* - T_{em}\left(k+1\right)\right| + \gamma\left|\psi_s^* - \psi_s\left(k+1\right)\right| \tag{14}$$

where $\psi_s = \psi_d + j\psi_q$ is the stator flux and γ the weighting factor.

The cost function in (10) or (14) is to be minimized based on eight voltage vectors $\left(V_0 - V_7\right)$ of a 2-level three-phase inverter to obtain the optimum voltage vector for the next control cycle as the following:

$$v_{opt} = \min_{i=0-7}\left(g_{MPCC}\, ?r\, g_{MPTC}\right) \tag{15}$$

III. Proposed MPC Methods

The proposed methods aim to improve the steady-state performance, regulate the switching frequency and eliminate the weighting factor while maintaining an overall performance trade-off.

Prior to discussing the proposed method, it is essential to consider the step delay compensation. In the conventional MPC, the machine variables are measured at time instant (k) and then predicted at time instant (*k*+1). However, the actuating signals (voltage vector) are only available at time instant (*k*+2). This creates a step time delay [32]. To compensate for this delay, the variables are predicted at time instant (*k*+2). Thus, the cost function of the conventional MPCC and MPTC in (10) and (14) are rewritten as [33]:

$$g_{MPTC} = \left|T_e^* - T_e\left(k+2\right)\right| + \gamma\left|\psi_s^? - \psi_s\left(k+2\right)\right| \tag{16}$$

$$g_{MPCC} = \left|i_d^* - i_d\left(k+2\right)\right| + \left|i_q^* - i_q\left(k+2\right)\right| \tag{17}$$

A. Method I: Two-Vector dimensionless FDM-MPTC

The most common issue in MPTC is the selection of the weighting factor. The cost function of MPTC in (16) contains two objective functions based on torque and flux. Each objective function has a different degree of importance, and torque and flux have different magnitudes and units. Thus, a weighting factor $\left(\gamma\right)$ must be included to balance the performance. The selection of the weighting factor is an ambiguous process, and a significant performance effect can be experienced if an inappropriate value is selected. MPTC with a cost function based on voltages or evaluating torque and flux cost functions separately are some methods used to eliminate the weighting factor. Our proposed two-vector MPTC can eliminate the weighting factor using fuzzy decision-making (FDM) to select the optimum switching vector.

Generally, choosing the weighting factor $\left(\gamma\right)$ requires the absolute importance of both torque and flux objective functions. However, FDM depends on the relative importance of each

objective function over another and can be chosen based on the decision maker's subjective and qualitative experience and judgment. Torque and flux objective functions in (16) can be rewritten individually as:

$$g_T = \left| T_e^* - T_e\left(k+2\right) \right| \tag{18}$$

$$g_\psi = \left| \psi_s^* - \psi_s\left(k+2\right) \right| \tag{19}$$

The proposed method utilizes two switching vectors over one control cycle. The torque objective function in (18) is evaluated separately based on eight voltage vectors ($V_0 - V_7$) of a 2-level three-phase inverter and minimized to obtain an optimum first voltage vector V_1. The second optimum voltage vector V_2 is obtained based on FDM using the torque and flux objective function in (18) and (19).

The torque and flux objective functions in (18) and (19) are evaluated based on eight voltage vectors $(V_0 - V_7)$ of a 2-level three-phase inverter, and then the final optimum voltage vector is determined using FDM. FDM is used where insufficient and incomplete data exist for the solution [34]. It is a bit different from the traditional fuzzy approach and has been introduced for MPC in [35] but not for the aim of eliminating the weighting factor and was applied for MPC in power converters [36] and induction motors [37]. To apply FDM in MPC, the specification of membership and decision functions are required. The linear membership function is the common form used in MPC. Therefore, a cost function is evaluated at different voltage vectors $g_i\left(V_s\right), \left(V_s = 0-7\right)$, the linear membership function $\mathrm{m_i}\left(\mathrm{V_s}\right)$ can be stated as follows:

$$\mathrm{m_i}\left(V_s\right) = \left(\frac{g_i^{max} - g_i\left(V_s\right)}{g_i^{max} - g_i^{min}} \right)^{R_i} \tag{20}$$

where R_i is a priority weight factor and can be determined based on the relative importance of each objective function. In [38], the numbers for various relative importance cases are listed and assigned depending on the priority importance of an objective function over the other. For the proposed method, an intermediate value of 2 is selected as the priority weight for both torque and flux objective functions. Hence, the membership function of the torque objective function $\mathrm{m_T}\left(V_s\right)$ and flux objective function $\mathrm{m}_\psi\left(V_s\right)$ can be represented as:

$$\mathrm{m_T}\left(V_s\right) = \left(\frac{g_T^{max} - g_T\left(V_s\right)}{g_T^{max} - g_T^{min}} \right)^2 \tag{21}$$

$$\mathrm{m}_\psi\left(V_s\right) = \left(\frac{g_\psi^{max} - g_\psi\left(V_s\right)}{g_\psi^{max} - g_\psi^{min}} \right)^2 \tag{22}$$

The cost functions of torque $g_T\left(V_s\right)$ and flux $g_\psi\left(V_s\right)$ are evaluated based on eight different voltage vectors $\left(V_s = 0-7\right)$. Then, using the obtained values, their maximum $\left(g_T^{max}, g_\psi^{max}\right)$, and minimum values ($g_T^{min}, g_\psi^{min}$) as in (21) and (22), the torque and flux membership functions ($\mathrm{m_T}, \mathrm{m}_\psi$) in the range of [0 1] are obtained. Thus, an optimum voltage vector can be selected by minimizing and maximizing a decision function as:

$$\mathrm{m_D}\left(V_s\right) = \min\left\{ m_T\left(V_s\right), m_\psi\left(V_s\right) \right\} \tag{23}$$

The optimum voltage vector V_{opt} is selected as:

$$V_{opt} = \max_{s=0-7}\left(\mathrm{m_D}\left(V_s\right)\right)^* \tag{24}$$

With the previously obtained vector V_1 by minimizing the torque cost function and making the optimum vector obtained in (24) as $V_{opt} = V_2$, this will result in two different voltage vectors (V_1, V_2). By computing the *dq* voltages components of each of these two vectors as:

$$u_{dq1} = u_{dq}\left(V_1\right) \tag{25}$$

$$u_{dq2} = u_{dq}\left(V_2\right) \tag{26}$$

The final reference voltage u_{dq}^{ref} is obtained as the combinations of the *dq* voltages components of two vectors with different duty cycles as:

$$u_{dq}^{ref} = \frac{t_1 \times u_{dq1}}{T_s} + \frac{\left(T_s - t_1\right) \times u_{dq2}}{T_s} \tag{27}$$

where T_s is the sampling time, and $t_1\ \left(0 < t_1 < T_s\right)$ is the time assigned for the first vector $\left(V_1\right)$. The duty cycle d_1 of V_1 is determined based on the torque error as:

$$d_1 = \left| \frac{T_e^* - T_e\left(k+2\right)}{C_T} \right| \tag{28}$$

where C_T is a positive constant value to be chosen to minimize the torque ripple.

Hence, the proposed FDM-MPTC can eliminate the weighting factor by transforming the torque and flux terms into dimensionless quantities using FDM and obtaining the optimum voltage vector with the factorless MPTC. To improve the steady-state performance and reduce torque ripple, a second vector obtained by evaluating the torque cost function is applied along with the optimum vector for each control cycle. This will improve the torque performance and reduce torque ripple because the second vector is obtained by evaluating the torque cost function and its duty cycle based on the torque error. If the torque ripple is high, the vector obtained from the torque cost function $\left(V_1\right)$ will be applied for a longer time to reduce torque ripple. Finally, to regulate the switching frequency and account for a trade-off between the steady-state performance, weighting factor, and switching frequency, PWM modulator-based space vector is used. The reference u_{dq}^{ref} in (27) is fed to the SVM PWM modulator; thus, the inverter's switching pulses with a regulated switching frequency are generated. Fig. 2 shows a block diagram of the proposed FDM-MPTC.

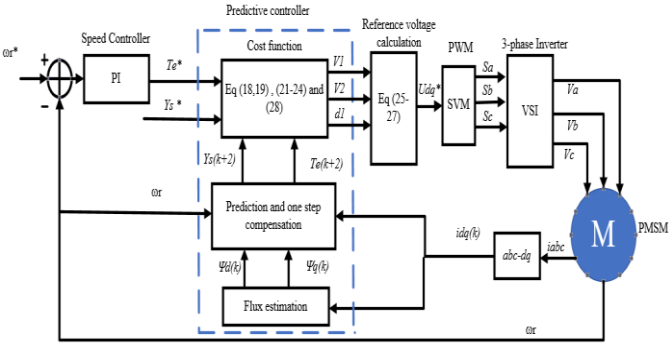

Fig.2. Proposed FDM-MPTC for PMSM drives.

B. *Method II: Two-vector FDM-MPCC*

The conventional MPCC evaluates the cost function in (17) based on the current difference to obtain the optimum switching vector for the next control cycle. Most improvement of MPCC applies one or more vectors along with the optimum vector over one control cycle. Usually, the weighting factor is not required in MPCC. However, weighting factors are used to render the cost functions comparable in magnitude and units. Clearly, the MPCC cost function terms have the same unit but may have different magnitudes. Thus, the weighting factor can be used, like in [39], which presented an MPCC cost function with a weighting factor computed using a fuzzy logic controller based on current errors. In the proposed MPCC (P-MPCC), two vectors with duty cycle control are applied over one control cycle. The first vector selected using FDM presented in method I by rewriting the cost function in (17) into two separate objective functions. The i_d current difference as the *d*-objective function and the i_q current difference as the *q*-objective function as follows:

$$g_d\left(V_s\right)=\left|i_d^{\,*}-i_d\left(k+2\right)\right| \tag{29}$$

$$g_q\left(V_s\right)=\left|i_q^{\,*}-i_q\left(k+2\right)\right| \tag{30}$$

The membership functions m_i for the current cost functions $g_d\left(V_s\right)$ and $g_q\left(V_s\right)$ can be expressed in the general form with different priority weights as:

$$\mathrm{m_i}\left(V_s\right)=\left(\frac{g_i^{max}-g_i\left(V_s\right)}{g_i^{max}-g_i^{min}}\right)^{R_i} \tag{31}$$

The priority weight R_i in (31) is determined based on the relative importance of each objective function. First, a pairwise comparison matrix Γ is constructed by comparing the objective function with each other. Since the current i_q directly influences the torque and current performance, the *q*-objective function is given moderate importance over the *d*-objective function to improve the torque performance. The comparison matrix Γ between the two objective functions $(\left(g_d, g_q\right)$ can be obtained :

$$\Gamma=\begin{bmatrix}1 & 3\\ \frac{1}{3} & 1\end{bmatrix} \tag{32}$$

By computing the eigenvector γ corresponding to the maximum value of the eigenvalues of Γ, the priority weight R_i can be expressed as:

$$R_i=\left[\,R_1\ldots.?R_i\,\right]=\frac{\gamma_{\mathrm{i}max?}}{\sum_{i=1}^{i}\gamma_{\mathrm{i}max?}} \tag{33}$$

In our case, the priority weight $R_i=\left[R_q\ R_d\right]$, which has been obtained as $R_q=0.75$ and $R_d=0.25$. More details on obtaining the comparison matrix and computing the priority weight can be found in [38]. The membership function of the *q*-objective function $\mathrm{m_q}\left(V_s\right)$, and the *d*-objective function $\mathrm{m}_d\left(V_s\right)$ can be represented as:

$$\mathrm{m_q}\left(V_s\right)=\left(\frac{g_q^{max}-g_q\left(V_s\right)}{g_q^{max}-g_q^{min}}\right)^{R_q} \tag{34}$$

$$\mathrm{m_d}\left(V_s\right)=\left(\frac{g_d^{max}-g_d\left(V_s\right)}{g_d^{max}-g_d^{min}}\right)^{R_d} \tag{35}$$

The *d*-objective function $g_d\left(V_s\right)$ and *q*-objective function $g_d\left(V_s\right)$ are evaluated based on eight different voltage vectors $\left(V_s=0-7\right)$. Then, using the obtained values, their maximum $\left(g_d^{max}, g_d^{max}\right)$ and minimum values (g_d^{min}, g_d^{min}) as in (34) and (35), the membership functions ($\mathrm{m_d}, \mathrm{m}_d$) in the range of [0 1] can be obtained. Thus, an optimum voltage vector can be selected by minimizing and maximizing a decision function as:

$$\mathrm{m_D}\left(V_s\right)=\min\left\{m_d\left(V_s\right), m_q\left(V_s\right)\right\} \tag{36}$$

Then, the first optimum vector is determined by maximizing the decision function in (36) as:

$$V_1=\max_{s=0-7}\left(\mathrm{m_D}\left(V_s\right)\right) \tag{37}$$

The second vector is determined by minimizing the cost function in (17) as:

$$V_2=\min_{s=0-7}\left(\mathrm{g_{MPCC}}\right);$$

By computing the *dq* voltage components of two vectors (V_1, V_2), the final reference voltage u_{dq} is obtained as the combinations of the *dq* voltages components of the two vectors with different duty cycles as:

$$u_{dq}^{ref}=\frac{t_1\times u_{dq1}}{T_s}+\frac{\left(T_s-t_1\right)\times u_{dq2}}{T_s} \tag{38}$$

The duty cycle d_1 of V_1 is determined based on i_q current error as:

$$d_1=\left|\frac{i_q^{\,*}-i_q\left(k+2\right)}{C_q}\right| \tag{39}$$

where C_q is a positive constant value to be chosen to optimize the torque and current ripples.

Similar to method I, a PWM modulator based SVM is used to regulate the switching frequency, where the u_{dq}^{ref} in (38) is fed

into the PWM modulator to generate the switching pulses. The block diagram of the proposed P-MPCC is shown in Fig.3.

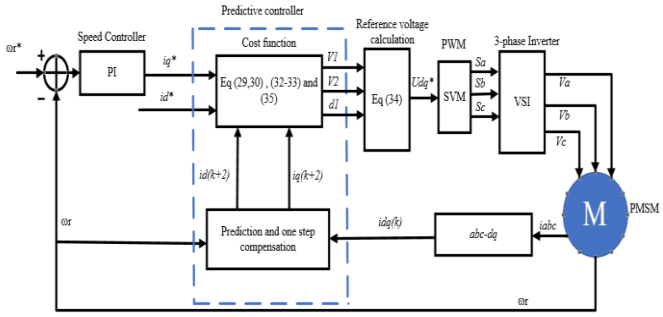

Fig.3.Proposed FDM-MPCC for PMSM drives

IV. Simulation Studies and Performance Analysis

In this section, the proposed two MPC methods (FDM-MPTC and FDM-MPCC) are designed and simulated using Matlab/Simulink based on a 1kW PMSM. To verify the effectiveness of these two methods, the conventional MPCs and two different existing MPC methods with similar approaches are also applied to the PMSM and compared with the proposed methods considering different characteristics. The proposed FDM-MPTC is to be compared with the conventional MPTC and an existing double vectors MPTC without weighing factor and based on voltage cost functions presented in [28]. The proposed FDM-MPCC is to be compared with the conventional MPCC and an existing two-vector MPCC presented in [23]. The PMSM parameters are kept the same for all simulations as in Table I, where the sampling frequency is set to 20 kHz, and the DC-link voltage is set to 200 V.

TABLE I
PMSM DRIVE PARAMETERS

Parameter	Symbol	Value and unit
Stator Resistance	R_s	0.47 Ω
d-Axis Inductance	L_d	14.2mH
q-Axis Inductance	L_q	15.9mH
Permanent magnet Flux	ψ_{pm}	0.1057 Wb
Number of Pole Pairs	P	3
Rated Speed	ω_n	1000 rpm
Rated Torque	T_n	2 Nm
dc-Link voltage	V_{DC}	200V
Inertia	J	0.002 kg/m^2
viscous Friction	B	0.0006 Nm/s
Sampling Time	T_s	50 µs

A. Proposed FDM-MPTC

The proposed FDM-MPTC and MPTC in [42] aim to eliminate the issues associated with the conventional MPTC by eliminating the weighting factor and using two vectors instead of one vector for one control cycle. Therefore, it is essential to carry out a comparative analysis of the conventional MPTC and the improved MPTC [28] to show the superiority of the proposed FDM-MPTC. For simplicity, the conventional MPTC and the existing MPTC in [28] will be referred to as MPTC- I and MPTC- II, respectively.

Fig. 4 shows the dynamic responses at 1000 rev/min (the rated speed) with an external load of 2 Nm applied at t = 0.1 s for MPTC- I, MPTC- II and the proposed FDM-MPTC. From top to bottom, the waveforms are the rotor speed, stator current, torque, and stator flux, respectively. As can be seen from the curves, the proposed FDM-MPTC shows an excellent dynamic response with lower overshoot and faster settling time compared to MPTC- I and MPTC- II In addition, it has smaller flux and torque ripples and smoother stator current response than MPTC- II. MPTC- I with a fixed value weighting factor and one switching vector for the whole control cycle shows the highest torque and flux ripples.

Fig.5 presents the waveforms of switching frequency, the harmonic spectra of stator currents, and the selected voltage vectors at the steady-state of 1000 rev/min (the rated speed) with a load torque of 2 Nm. It is seen that the proposed FDM-MPTC shows an almost fixed switching frequency with an average value of 4.8 kHz, which is better and more regulated than MPTC- II with an average switching frequency of 5.1 kHz. On the other hand, MPTC-I has an unregulated switching frequency with an average value of 7.4 kHz. This is because the switching pulses are directly generated in MPTC- I without a PWM modulator. In addition, the total harmonic distortion (THD) of the stator current is calculated up to 6 kHz maximum frequency. The THD of the proposed FDM-MPTC is only 4.61%, less than 5.12% of MPTC- II. MPTC- I has a broad harmonic spectrum, and the stator current THD is up to 6.31%, much higher than the other two MPTC methods.

In addition to the good performance obtained by FDM-MPTC, its switching frequency is lower than the MPTC-II and MPTC-I methods. The quantitative comparison between them during the transient response and at the steady-state of 1000 rev/min with a load of 2 Nm is listed in Table II, including the settling time t_s, average switching frequency f_{avg}, torque ripple T_{rip}, flux ripple ψ_{rip}, and stator current THD. The average switching frequency f_{avg} is computed as $f_{avg} = 20N/6$, where N is the total switching instants of the six legs of a two-level inverter during a fixed period of 0.05 s. It can be concluded that the proposed FDM-MPTC has a superior performance in terms of torque and flux ripples and stator current THD, while its average switching frequency f_{av} is 94% and 64.8% of that of MPTC-II and MPTC- I, respectively. This emphasizes its superiority in reducing torque and stator flux ripples with less switching frequency and lower stator current THD. In conclusion, MPTC-II has better performance over the MPTC-I, and the proposed FDM-MPTC is capable of producing better performance than both MPTC-I and MPTC-II when tested under similar operating conditions and using the same parameters.

TABLE II
Numerical Comparisons of MPTC- I, MPTC- II [28], and the Proposed FDM-MPTC

Property / Method	t_s (s)	T_{ripp} (Nm)	ψ_{ripp} (Wb)	f_{avg} (Hz)	THD of i_a
MPTC- I	0.0441	0.1953	0.0062	7.4k	6.31%
MPTC- I I	0.0325	0.1435	0.0044	5.1k	5.12%
FDM-MPTC	0.0305	0.1241	0.0038	4.8k	4.61%

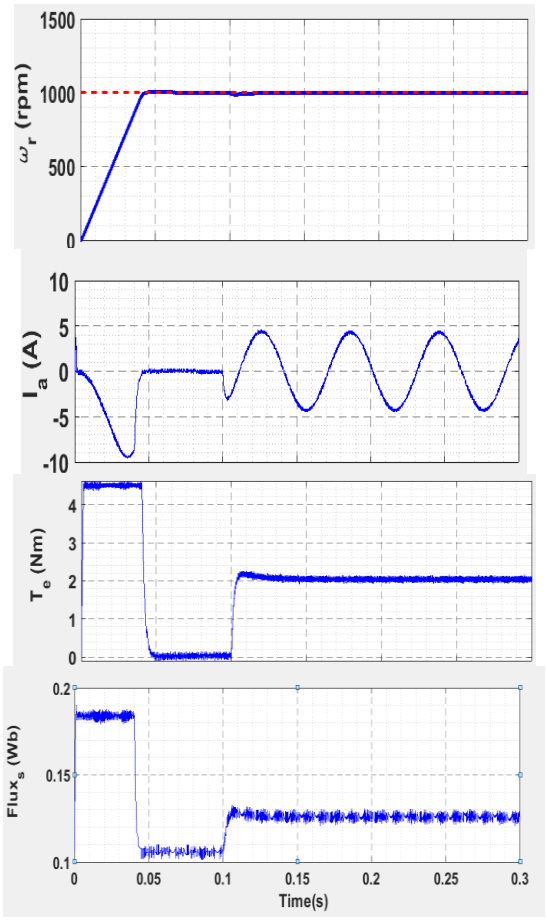

(a)

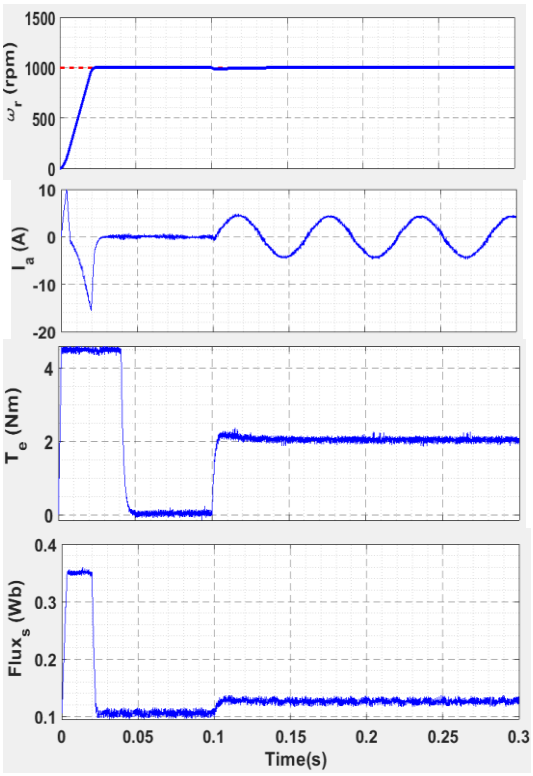

(b)

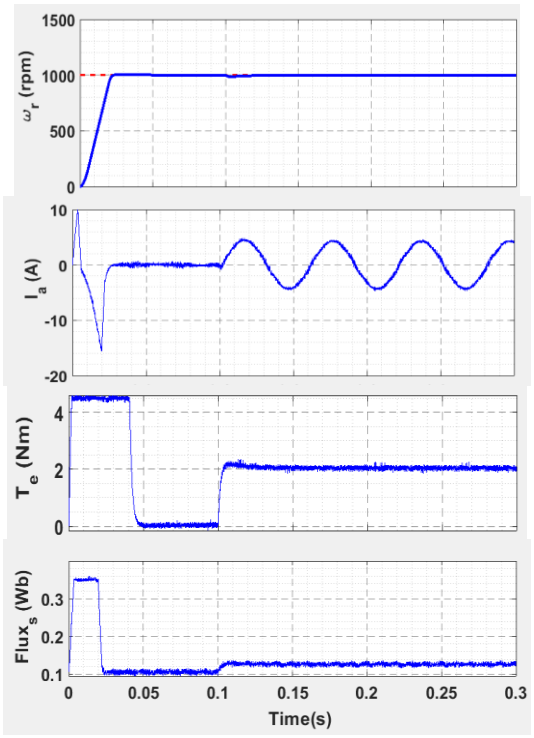

(c)

Fig.4. Responses of rotor speed, stator current, torque, and stator flux at 1000 r/min with sudden load change for (a) MPTC-I, (b) MPTC- II [28], (c) proposed FDM-MPTC.

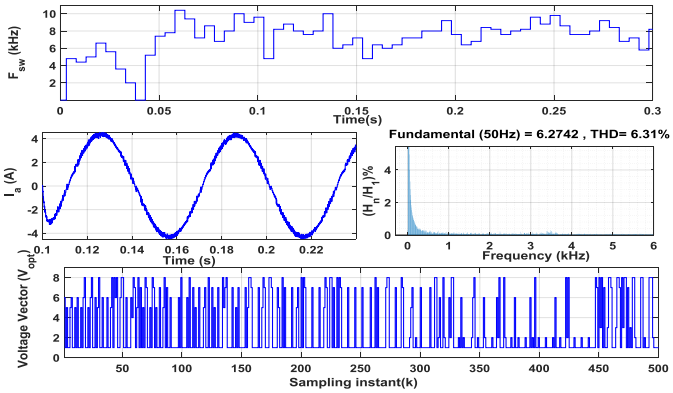

(a)

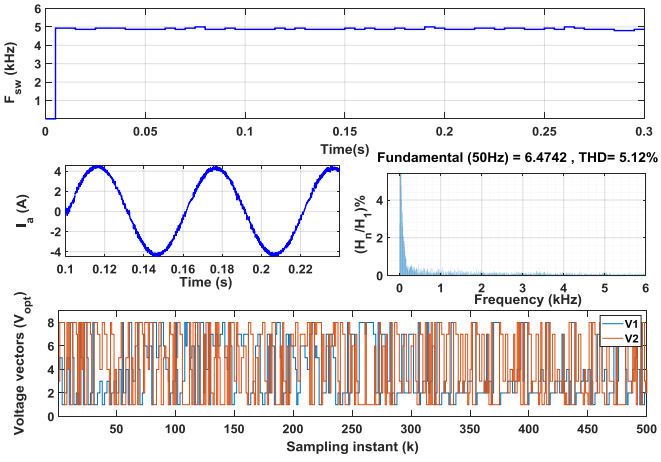

(b)

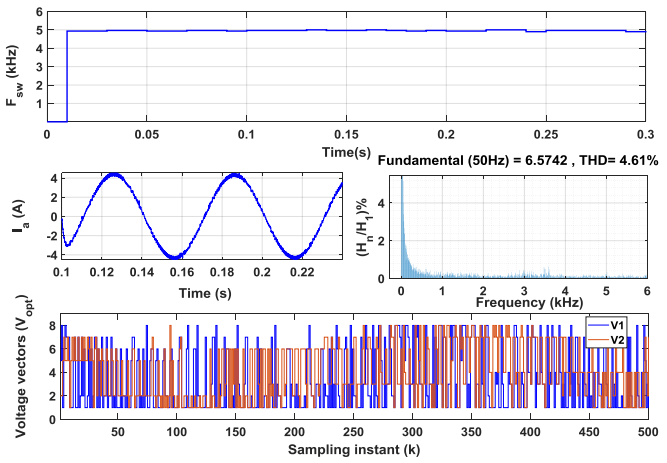

(c)

Fig.5. Switching frequency, the harmonic spectrum of stator current, and selected switching vectors for (a) MPTC- I, (b) MPTC-II [28], (c) proposed FDM-MPTC.

B. Proposed FDM-MPCC

Similar to the proposed FDM-MPTC, in order to validate the effectiveness and superiority of the proposed FDM-MPCC, performance comparisons are carried out with the conventional MPCC (MPCC-I) and an existing two-vector MPCC in [23] (MPCC-II), including dynamics and steady-state performance in terms of the settling time, torque and flux ripples, stator current THD, and switching frequency.

Fig.6 shows the dynamic response from standstill to 1000 rev/m (the rated speed) and the steady-state response with a sudden 2 Nm load applied at 0.1 s for MPCC-I, MPCC-II, and proposed FDM-MPCC. The waveforms from top to bottom are the rotor speed response, stator current, torque, and flux. Based on the rotor speed response, the proposed FDM-MPCC has a faster settling time and lower overshoot than the other two methods. The stator current of FDM-MPCC is more sinusoidal and less distorted. The torque and flux ripples are much reduced for FDM-MPCC compared to MPCC-I and MPCC-II.

Fig.7 illustrates the switching frequency, harmonics spectra, and the selected switching vectors for three methods. Generally, MPCC-I has a very high variable switching frequency due to the direct generation of switching pulses and the absence of any regulation technique. MPCC-II has a better switching frequency with an average value of 5.68 kHz. The proposed FDM-MPCC shows a regulated frequency with a lower average value of 4.26 kHz, which is only 75% of that of MPCC-II with the same sampling frequency. Moreover, the stator current THD is calculated up to 6 kHz maximum frequency, and the proposed FDM-MPCC recorded the lowest THD of 4.12% compared to 4.71% and 5.51% for MPCC-II and MPCC-I, respectively.

The numerical comparison of FDM-MPCC with the other two methods is listed in Table III, which shows the superiority of the proposed method with low torque and flux ripples, less THD, low switching frequency, and faster dynamic response.

Apart from this, comparing MPCC methods in this section with the MPTC methods from the previous section shows that MPCC methods record better stator current performance with less THD, and torque ripple increased for MPCC-I and MPCC-II compared to those MPTC methods. This is because the cost function in MPCC is evaluated based on current, while in MPTC, it is evaluated based on torque and flux. However, the proposed FDM-MPCC has produced high quality current response and maintained a good torque response with less ripples comparable to the proposed FDM-MPTC. This is because the second vector is selected based on FDM with high priority given to the q-objective function in FDM-MPCC. Also the i_q error is used to calculate the duty cycle of the second vector to minimize the torque ripple.

Finally, the proposed FDM-MPCC has shown superior performance over the other MPCC methods and can maintain a good balance for optimal overall performance, including good current quality, regulated switching frequency, and reduced torque ripple.

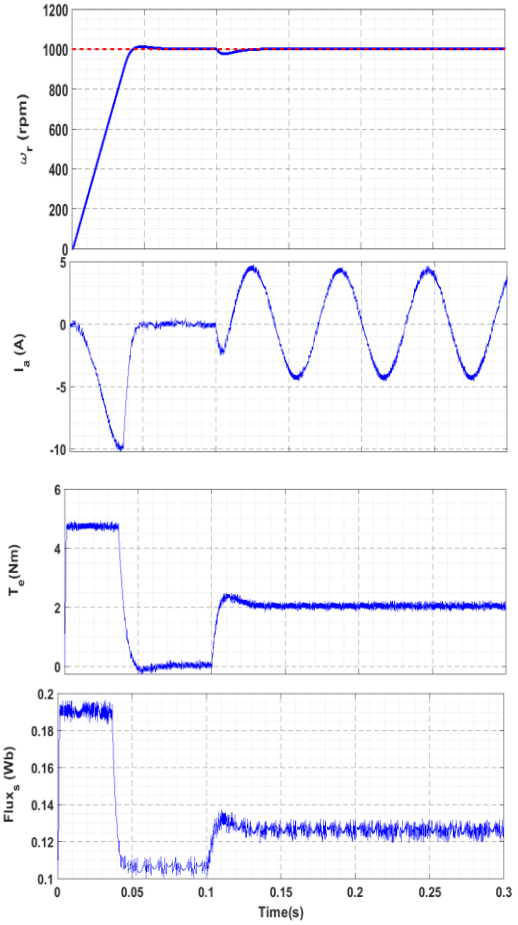

(a)

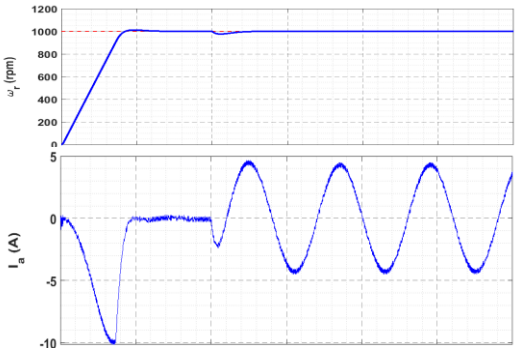

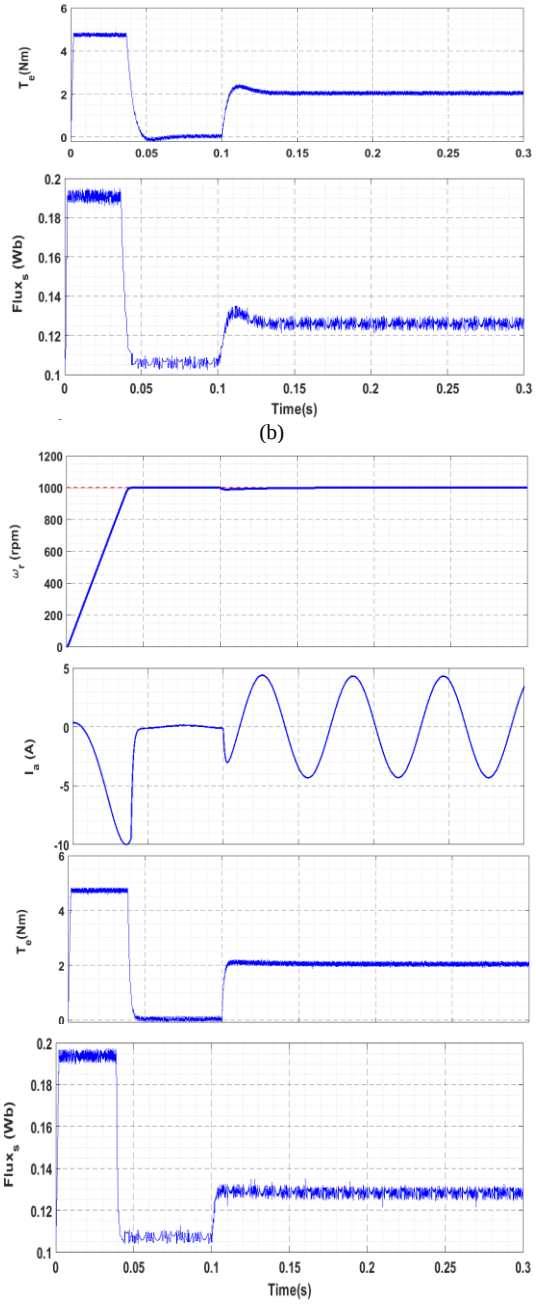

Fig.6. Response of rotor speed, stator current, and torque and stator flux at 1000 r/min with sudden load change for (a) MPCC-I, (b) MPCC- II [23], (c) proposed FDM-MPCC.

TABLE III
NUMERICAL COMPARISONS OF MPCC- I, MPCC- II [23], AND THE PROPOSED FDM-MPTC

Property / Method	t_s (s)	T_{ripp} (N.m)	ψ_{ripp} (Wb)	f_{avg} (Hz)	THD of i_a
MPCC- Ⅰ	0.0427	0.2026	0.0052	6.13k	5.51%
MPCC- Ⅰ Ⅰ	0.0421	0.1510	0.0043	5.68k	4.71%
FDM-MPCC	0.0393	0.1283	0.0028	4.26k	4.12%

V. CONCLUSION

The unsatisfactory steady-state performance, unregulated switching frequency, and ambiguous process of weighting factor selection made conventional MPC methods less effective than traditional control methods for AC machine drives. Thus,

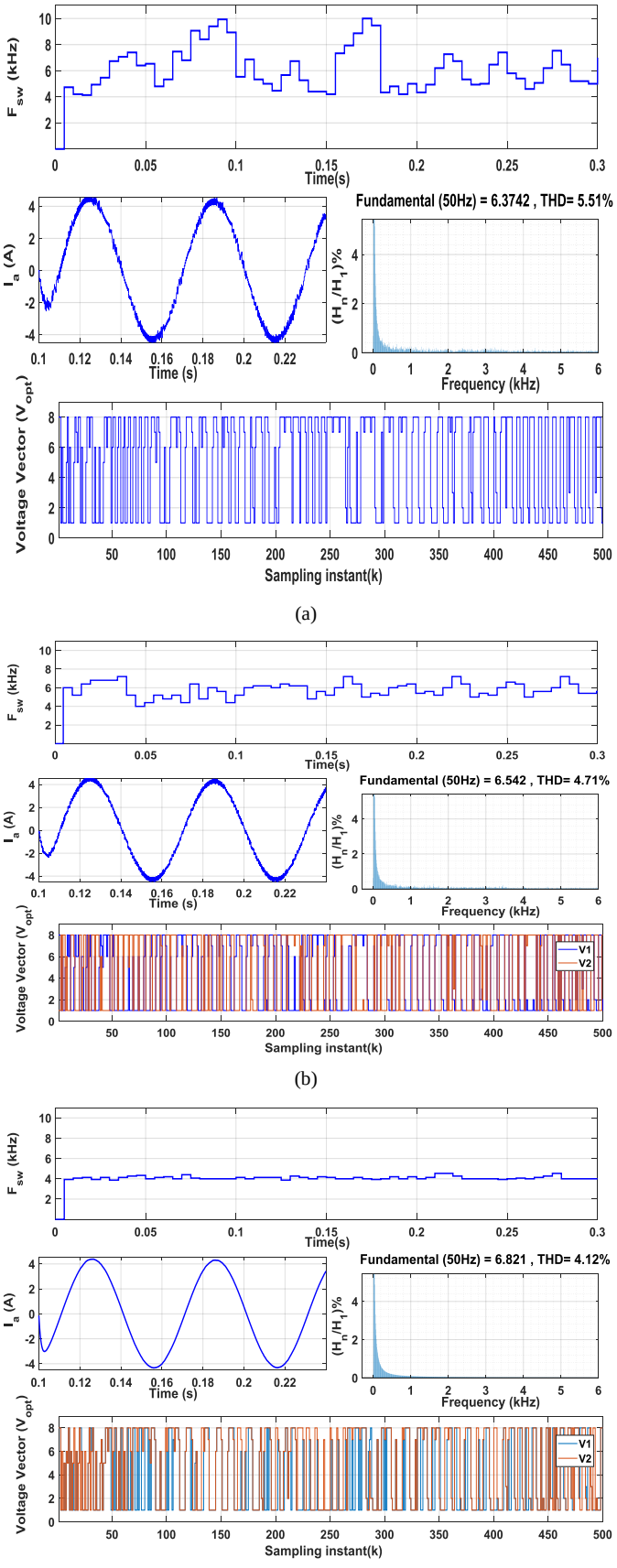

Fig.7. Switching frequency, the harmonic spectrum of stator current, and selected switching vectors for (a) MPCC- Ⅰ , (b) MPCC- II [23], (c) proposed FDM-MPCC.

various improvements, such as two or more vectors during one control cycle, weighting factor eliminations, and switching frequency regulation techniques, were implemented to maintain the effectiveness of MPCs. This paper proposed two MPC methods based on predictive torque &flux and current controls to reduce the torque ripple, regulate switching frequency, and maintain good current quality. The proposed methods utilize two vectors for one control cycle and eliminate the issue of weighing factors using FDM. Compared with the conventional MPCs and similar existing improved MPCs, the proposed methods have shown superiority in terms of different characteristics under transient and steady-state conditions. The proposed FDM-MPCC has shown better current response and maintained reduced current ripples compared to the proposed FDM-MPTC. The conventional and existing MPCCs have shown slight improvement in the current responses, but their torque ripples are higher than those of MPTC-based methods, emphasizing the proposed method's superiority and ability to balance for optimal overall performance.

REFERENCES

[1] B. K. Bose, "Adjustable speed AC drives—A technology status review," *Proceedings of the IEEE*, vol. 70, no. 2, pp. 116-135, 1982.

[2] K. Wang, Y. Li, Q. Ge, and L. Shi, "An Improved Indirect Field-Oriented Control Scheme for Linear Induction Motor Traction Drives," *IEEE Transactions on Industrial Electronics*, vol. 65, no. 12, pp. 9928-9937, 2018.

[3] Z. Zhang, R. Tang, B. Bai, and D. Xie, "Novel Direct Torque Control Based on Space Vector Modulation With Adaptive Stator Flux Observer for Induction Motors," *IEEE Transactions on Magnetics*, vol. 46, no. 8, pp. 3133-3136, 2010.

[4] Y. N. Tatte and M. V. Aware, "Torque Ripple and Harmonic Current Reduction in a Three-Level Inverter-Fed Direct-Torque-Controlled Five-Phase Induction Motor," *IEEE Transactions on Industrial Electronics*, vol. 64, no. 7, pp. 5265-5275, 2017.

[5] S. Vazquez *et al.*, "Model predictive control: A review of its applications in power electronics," *IEEE industrial electronics magazine*, vol. 8, no. 1, pp. 16-31, 2014.

[6] J. Rodriguez *et al.*, "State of the art of finite control set model predictive control in power electronics," *IEEE Transactions on Industrial Informatics*, vol. 9, no. 2, pp. 1003-1016, 2012.

[7] A. A. Ahmed, B. K. Koh, H. S. Park, K. Lee, and Y. I. Lee, "Finite-Control Set Model Predictive Control Method for Torque Control of Induction Motors Using a State Tracking Cost Index," *IEEE Transactions on Industrial Electronics*, vol. 64, no. 3, pp. 1916-1928, 2017.

[8] A. A. Ahmed, B. K. Koh, and Y. I. Lee, "A Comparison of Finite Control Set and Continuous Control Set Model Predictive Control Schemes for Speed Control of Induction Motors," *IEEE Transactions on Industrial Informatics*, vol. 14, no. 4, pp. 1334-1346, 2018.

[9] W. Xie *et al.*, "Finite-Control-Set Model Predictive Torque Control With a Deadbeat Solution for PMSM Drives," *IEEE Transactions on Industrial Electronics*, vol. 62, no. 9, pp. 5402-5410, 2015.

[10] E. Fuentes, C. A. Silva, and R. M. Kennel, "MPC Implementation of a Quasi-Time-Optimal Speed Control for a PMSM Drive, With Inner Modulated-FS-MPC Torque Control," *IEEE Transactions on Industrial Electronics*, vol. 63, no. 6, pp. 3897-3905, 2016.

[11] X. Li and P. Shamsi, "Model Predictive Current Control of Switched Reluctance Motors With Inductance Auto-Calibration," *IEEE Transactions on Industrial Electronics*, vol. 63, no. 6, pp. 3934-3941, 2016.

[12] M. Preindl, "Robust Control Invariant Sets and Lyapunov-Based MPC for IPM Synchronous Motor Drives," *IEEE Transactions on Industrial Electronics*, vol. 63, no. 6, pp. 3925-3933, 2016.

[13] F. Wang, S. Li, X. Mei, W. Xie, J. Rodríguez, and R. M. Kennel, "Model-Based Predictive Direct Control Strategies for Electrical Drives: An Experimental Evaluation of PTC and PCC Methods," *IEEE Transactions on Industrial Informatics*, vol. 11, no. 3, pp. 671-681, 2015.

[14] M. Siami, D. A. Khaburi, M. Rivera, and J. Rodríguez, "An Experimental Evaluation of Predictive Current Control and Predictive Torque Control for a PMSM Fed by a Matrix Converter," *IEEE Transactions on Industrial Electronics*, vol. 64, no. 11, pp. 8459-8471, 2017.

[15] J. Retif, L.-S. Xuefang, and F. Morel, "Predictive Current Control for an Induction Motor," in *2008 IEEE Power Electronics Specialists Conference*, pp. 3463-3468, 2008.

[16] L. Sheng, D. Li, and Y. Ji, "Two-Vector FCS-MPC for Permanent-Magnet Synchronous Motors Based on Duty Ratio Optimization," *Mathematical Problems in Engineering*, vol. 2018, p. 9061979, 2018.

[17] B. Li, X. Ling, Y. Huang, L. Gong, and C. Liu, "An Improved Model Predictive Current Controller of Switched Reluctance Machines Using Time-Multiplexed Current Sensor," (in eng), *Sensors (Basel)*, vol. 17, no. 5, p. 1146, 2017.

[18] Y. Zhang and J. Cortés, "Model predictive control for transient frequency regulation of power networks," *Automatica*, Vol. 123,p. 109335.

[19] T. Dragičević and M. Novak, "Weighting Factor Design in Model Predictive Control of Power Electronic Converters: An Artificial Neural Network Approach," *IEEE Transactions on Industrial Electronics*, vol. 66, no. 11, pp. 8870-8880, 2019.

[20] Y. Zhang and H. Yang, "Two-Vector-Based Model Predictive Torque Control Without Weighting Factors for Induction Motor Drives," *IEEE Transactions on Power Electronics*, vol. 31, no. 2, pp. 1381-1390, 2016.

[21] Y. Liu, S. Cheng, Y. Zhao, J. Liu, and Y. Li, "Optimal two-vector combination-based model predictive current control with compensation for PMSM drives," *International Journal of Electronics*, vol. 106, no. 6, pp. 880-894, 2019.

[22] H. Lin and W. Song, "Three-Vector Model Predictive Current Control of Permanent Magnet Synchronous Motor Based on SVM," *IEEE International Symposium on Predictive Control of Electrical Drives and Power Electronics (PRECEDE)*, pp. 1-6,2019.

[23] Y. Zhang, L. Huang, D. Xu, J. Liu, and J. Jin, "Performance evaluation of two-vector-based model predictive current control of PMSM drives," *Chinese Journal of Electrical Engineering*, vol. 4, no. 2, pp. 65-81, 2018.

[24] P. Cortes *et al.*, "Guidelines for weighting factors design in Model Predictive Control of power converters and drives," in *2009 IEEE International Conference on Industrial Technology*, pp. 1-7, 2009.

[25] C. A. Rojas, J. Rodriguez, F. Villarroel, J. Espinoza, and D. A. Khaburi, "Multiobjective Fuzzy Predictive Torque Control of an induction motor drive," in *The 6th Power Electronics, Drive Systems & Technologies Conference (PEDSTC2015)*, pp. 201-206, 2015.

[26] P. Zanchetta, "Heuristic multi-objective optimization for cost function weights selection in finite states model predictive control," in *2011 Workshop on Predictive Control of Electrical Drives and Power Electronics*, pp. 70-75, 2011.

[27] M. Mamdouh, M. A. Abido, and Z. Hamouz, "Weighting Factor Selection Techniques for Predictive Torque Control of Induction Motor Drives: A Comparison Study," *Arabian Journal for Science and Engineering*, vol. 43, no. 2, pp. 433-445, 2018.

[28] X. Zhang and B. Hou, "Double Vectors Model Predictive Torque Control Without Weighting Factor Based on Voltage Tracking Error," *IEEE Transactions on Power Electronics*, vol. 33, no. 3, pp. 2368-2380, 2018.

[29] X. Zhang, B. Hou, Y. He, and D. Gao, "Model predictive torque control of surface mounted permanent magnet synchronous motor drives with voltage cost functions," *Journal of Power Electronics*, vol. 18, no. 5, pp. 1369-1379, 2018.

[30] I. Jlassi and A. J. M. Cardoso, "Lookup-Table-Based Model Predictive Torque Control Without Weighting Factors for PMSM Drives," in *IECON 2019 - 45th Annual Conference of the IEEE Industrial Electronics Society*, vol. 1, pp. 1165-1170, 2019.

[31] U. Ammann, R. Vargas, and J. Roth-Stielow, "Investigation of the average switching frequency of Direct Model Predictive Control converters," in *2010 IEEE International Conference on Industrial Technology*, pp. 1800-1807, 2010.

[32] P. Cortes, J. Rodriguez, C. Silva, and A. Flores, "Delay compensation in model predictive current control of a three-phase inverter," *IEEE Transactions on Industrial Electronics*, vol. 59, no. 2, pp. 1323-1325,

2011.

[33] Z. Yongchang and W. Xianglong, "Torque ripple RMS minimization in model predictive torque control of PMSM drives," in *2013 International Conference on Electrical Machines and Systems (ICEMS)*, pp. 2183-2188, 2013.

[34] K. Cengiz, O. Sezi Cevik, and O. Basar, "Fuzzy Multicriteria Decision-Making: A Literature Review," *International Journal of Computational Intelligence Systems*, vol. 8, no. 4, pp. 637-666, 2015.

[35] J. M. d. C. Sousa and U. Kaymak, "Model predictive control using fuzzy decision functions," *IEEE Transactions on Systems, Man, and Cybernetics, Part B (Cybernetics)*, vol. 31, no. 1, pp. 54-65, 2001.

[36] F. Villarroel, J. R. Espinoza, C. A. Rojas, J. Rodriguez, M. Rivera, and D. Sbarbaro, "Multiobjective Switching State Selector for Finite-States Model Predictive Control Based on Fuzzy Decision Making in a Matrix Converter," *IEEE Transactions on Industrial Electronics*, vol. 60, no. 2, pp. 589-599, 2013.

[37] C. A. Rojas, J. R. Rodriguez, S. Kouro, and F. Villarroel, "Multiobjective Fuzzy-Decision-Making Predictive Torque Control for an Induction Motor Drive," *IEEE Transactions on Power Electronics*, vol. 32, no. 8, pp. 6245-6260, 2017.

[38] V. Kumar, P. Gaur, and A. P. Mittal, "Finite-state model predictive control of NPC inverter using multi-criteria fuzzy decision-making," *International Transactions on Electrical Energy Systems*, vol. 25, no. 5, pp. 876-897, 2015.

[39] H. Mahmoudi, M. Aleenejad, P. Moamaei, and R. Ahmadi, "Fuzzy adjustment of weighting factor in model predictive control of permanent magnet synchronous machines using current membership functions," in *2016 IEEE Power and Energy Conference at Illinois (PECI)*, pp. 1-5, 2016.

Nabil Farah (Graduate Student Member, IEEE) received his bachelor's degree and master's degree in electrical engineering in 2015 and 2018, respectively, and currently, he is working toward a Ph.D. degree in electrical engineering as well at the University of Technology Sydney, NSW, Australia.

His research interests include electrical machine drives control and optimization and predictive control methods for PMSMs drives.

Gang Lei (M'14) received a B.S. degree in Mathematics from Huanggang Normal University, China, in 2003, the M.S. degree in Mathematics, and a Ph.D. degree in Electrical Engineering from Huazhong University of Science and Technology, China, in 2006 and 2009, respectively.

He is currently a lecturer at the School of Electrical and Data Engineering, University of Technology Sydney (UTS), Australia. His current research interests include electrical machines and systems, multidisciplinary design optimization, industrial big data, and cloud computing techniques.

Jianguo Zhu (S'93–M'96–SM'03) received the B.E. degree from Jiangsu Institute of Technology, China, in 1982, the M.E. degree from Shanghai University of Technology, China, in 1987, and the Ph.D. degree from the University of Technology, Sydney (UTS), Australia, in 1995, all in electrical engineering.

He is currently a professor of Electrical Engineering at the University of Sydney, Australia. His research interests include electromagnetics, magnetic properties of materials, electrical machines and drives, power electronics, and green energy systems.

Youguang Guo (Senior Member, IEEE) received the B.E. degree from Huazhong University of Scienceand Technology, Wuhan, China, in 1985, the M.E.degree from Zhejiang University, Hangzhou, China,in 1988, and the Ph.D. degree from the University of Technology Sydney (UTS), Sydney, NSW, Australia, in 2004, all in electrical engineering. He is currently a Professor at the School of Electrical and Data Engineering, UTS. His research fields include the measurement and modeling of properties of magnetic materials, numerical analysis of electromagnetic field, electrical machine design optimization, and power electronic drives and control.